Special issue of the 2nd International Conference on Computational and Experimental Science and Engineering (ICCESEN 2015)

Influence of Rare Earth Element on the Mechanical Properties of ZE41 Magnesium Alloys Produced by Mechanical Alloying

O. Sahin*, F. Haluk Ertsak, K. Oztekin, S. Ozarslan
Mustafa Kemal University, Science and Art Faculty, Micro/Nanomechanic Characterization Laboratory, Hatay 31034, Turkey

In this work, we have intended to synthesize ZE41 Magnesium alloys having varying content of Ce of 0.3, 0.6 and 0.9 wt.% and to investigate mechanical properties of these alloys. Alloys were produced by mechanical alloying under argon atmosphere. Structural, and mechanical properties of these alloys were investigated by means of XRD, SEM and nanoindenter analysis. From the XRD data it is found that as the Ce content increases, the crystallite size also increases. On the other hand, the hardness of the alloys decreases with the increasing Ce content. Indentation results show that the measured hardness displays a peak load dependence. Load-independent hardness was calculated by Hays-Kendall approach. As a results, it was found that Ce-doping modifies the microstructure and hardness of the alloy.

DOI: 10.12693/APhysPolA.130.289
PACS/topics: 62.20.–x, 62.20.Fe, 62.20.Qp

1. Introduction

Magnesium alloys offer an incomparable combination of physical and mechanical properties, like high strength-to-weight ratio, good damping capacity and admirable machinability, which are correctly exploited in designing magnesium-based consumer products. The automobile industry is one of the major industries, which has been taking advantage from the development in the field of magnesium research. Reducing automobile weight is vital in order to reduce the fuel consumption and exhaust emission and hence the automakers are progressively making use of light weight magnesium alloys [1–3].

Mechanical alloying (MA) is a powder processing technique that allows production of homogeneous materials starting from blended elemental powder mixtures. John Benjamin and his colleagues at the Paul D. Merica Research Laboratory of the International Nickel Company (INCO) have developed the process around 1966 [4]. Different types of high-energy milling equipment are used to produce mechanically alloyed powders. They differ in their capacity, efficiency of milling and additional arrangements for cooling, heating, etc. [4, 5].

Nanoindentation has been widely used for characterization of the nanomechanical properties of nanomaterials [6, 7], and thin films [8–10], because of its high sensitivity and the excellent resolution for obtaining the nanohardness, elastic modulus and the elastic/plastic deformation behaviour in a relatively easy fashion [11].

In this study, in order to investigate mechanical properties of ZE41 Mg alloys, we have produced for the first time the alloys having different Ce concentrations, using mechanical alloying method. According to our best knowledge, there are no reports on the production and mechanical properties of Ce-doped ZE41 Mg alloys. Therefore, ZE41 Mg alloys were produced by using mechanical alloying and mechanical properties of ZE41 Mg alloys were analyzed using nanoindentation method.

2. Experimental procedure

ZE41 Mg alloys were doped with 0.3, 0.6, and 0.9 wt.% of Ce. ZE41 magnesium alloys were produced by mechanical alloying method. Milling speed was 300 rpm, the ball-to-powder ratio was 20:1 and milling time was 12 hours. In order to prevent oxidation, the ZE41 Mg alloys were kept in the glove box compartment. Stearic acid 2 wt.% was added to prevent sudden flocculation of the samples. After the milling, the stearic acid was evaporated from these powders, which then were pressed. Pressed samples were sintered at 400 °C for nanohardness tests. Nanohardness testing of samples was performed by using Hysitron Triboindenter TI-950 with Berkovich tip. Hardness tests of samples was done by using loads from 1000 μN to 10000 μN. Mechanical properties of samples were analyzed with Oliver-Pharr method [12]. Hardness definition in Oliver-Pharr method is

$$H_{\text{nano}} = \frac{P_{\max}}{A_{\text{c}}}, \quad (A_{\text{c}} = 24.5h_{\text{c}}^2). \tag{1}$$

Here $P_{\max}$ is maximum test load and A_{c} is the contact area. Contact depth in Oliver-Pharr method can be calculated using Eq. (2);

$$h_{\text{c}} = h_{\max} - \beta\frac{P_{\max}}{S}, \tag{2}$$

$$S = \frac{\mathrm{d}P}{\mathrm{d}h}, \tag{3}$$

where β is an indenter geometry-dependent constant. It has been shown that β has an empirical value of 0.72 for the Berkovich indenter. S is the unloading contact stiffness. The detailed methodology can be found in the literature [12, 13].

*corresponding author; e-mail: sduosman@gmail.com

3. Results and discussion

Nanoindentation was employed to analyze the mechanical properties of pure and Ce-doped ZE41 magnesium alloys. Figure 1 shows applied indentation test load vs. penetration depth curves for pure and Ce-doped (0.3, 0.6, and 0.9 wt.%) samples. All indentation curves, given in Fig. 1 were analysed using Oliver-Pharr procedure. These curves have a smooth and regularly shape. We can clearly say that these alloys exhibit elastoplastic behaviour. The inset in the Fig. 1 shows the SPM micrograph of the ZE41 alloys. From the micrograph it is seen that ZE41 sample surfaces are homogeneous and without cracks. Also, since the Berkovich indenter shape is exactly the same as the indentation shape observed on the sample surface, we can say that there is no significant surface finishing effect. Thus, it is considered to be unnecessary to discuss the effect of microcracking on the nanohardness measurements in this study. A cross-section image is given Fig. 1b. There is no pile-up and sink-in behaviour of the examined alloys.

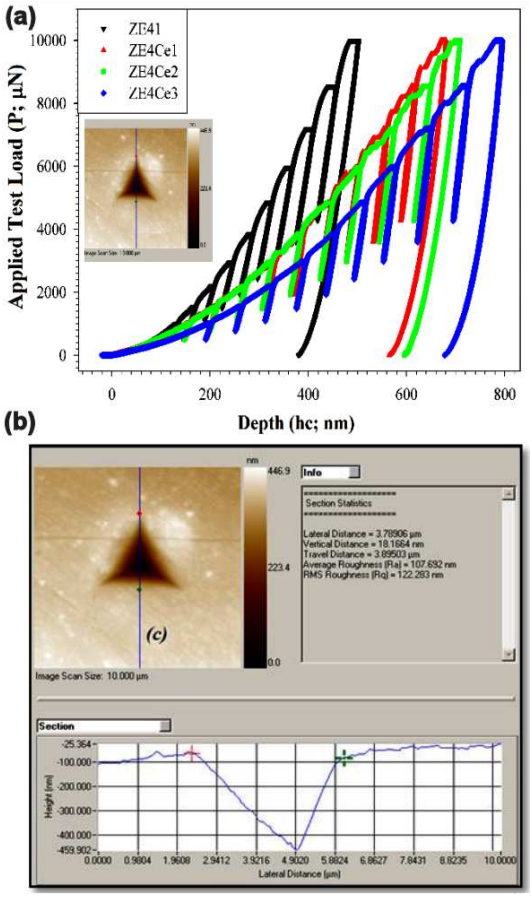

Fig. 1. (a) Applied indentation test load versus indentation depth graph of ZE41 alloys, (b) SPM cross-section image of one indent.

The morphology and microstructure of the ZE41 Mg alloys were examined by scanning electron microscopy (SEM). Figure 2 shows that all examined alloys are fully covered by Mg particles. The average particle size of the alloys was measured by a pixel analyzing program. The distribution of particles is roughly homogeneous and their diameters are 35, 28, 30 and 31 μm, respectively. Particle sizes of these alloys have first decreased at Ce content of 0.3 wt.% and then increased at higher Ce content.

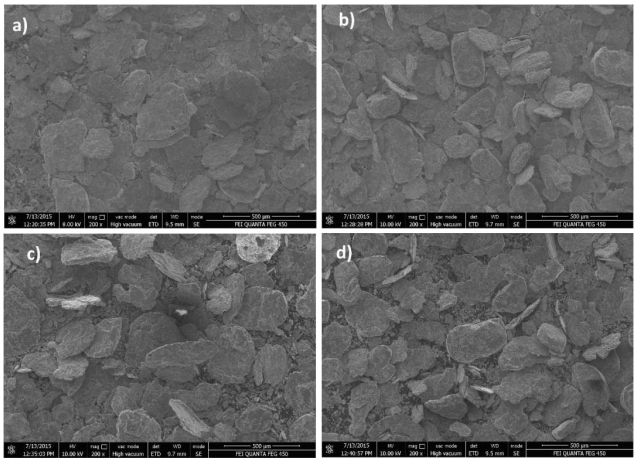

Fig. 2. SEM images of (a) ZE41, (b) ZE41-0.3Ce, (c) ZE41-0.6Ce, (d) ZE41-0.9Ce.

The structural properties of the un-doped and Ce-doped ZE41 Mg alloys were determined by XRD measurements. Figure 3 shows the typical XRD patterns of the ZE41 Mg alloys with different Ce concentrations. Preferential orientations are (110), (101) and (103). On the other hand, the intensities of the (111) peaks have decreased with the increasing Ce concentration.

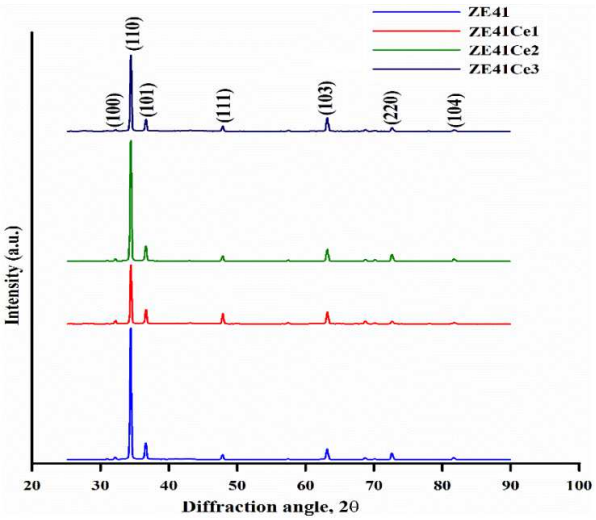

Fig. 3. XRD patterns of un-doped and Ce-doped ZE41 Mg alloys.

Average crystallite size of alloys was calculated using Debye-Scherrer's formula given in Eq. (4). Micro-strain ε and dislocation density ρ can be calculated using Eq. (5) and Eq. (6), respectively.

$$D = \frac{0.94\lambda}{\beta \cos\theta}. \tag{4}$$

$$\varepsilon = \frac{\beta \cos\theta}{4}. \tag{5}$$

$$\rho = \frac{15\varepsilon}{aD}. \tag{6}$$

The calculated values are given in Table I. From this analysis, crystallite size in the ZE41 Mg alloys increases from 57.06 to 75.16 nm with the increasing Ce amount. On the other hand, dislocation density decreases with the increasing Ce amount.

TABLE I

XRD analysis of ZE41 alloys [14].

Sample name	Ce concentration [wt.%]	FWHM	ε	ρ [cm$^{-2}\times10^{14}$]	D [nm]
ZE41	0	0.176	6.7×10^{-4}	9.15	57.06
ZE41Ce1	0.3	0.151	5.7×10^{-4}	6.61	66.46
ZE41Ce2	0.6	0.136	5.2×10^{-4}	5.45	72.51
ZE41Ce3	0.9	0.130	4.9×10^{-4}	4.82	75.16

There is a correlation between the hardness and dislocation density of a crystal. According to this, hardness definition of a material is the resistance to the dislocation motion. Occurrence of this increase may be due to both pinning of dislocations at the impurity sites and other defects, caused by the presence of impurity atoms in the crystal, and also to variation in the magnitude of the binding forces in the crystal containing impurities. It was seen that the nanohardness plateau values have decreased with increasing Ce content. It implies that hindering of motion of dislocations is a critical issue in hardening of the ZE41 Mg alloys. This situation is in agreement with the studies by Sahin et al. [15].

Nanohardness (H_{N}) values at each imposed depth were calculated using Eq. (1). The peak indentation test load dependence of nanohardness data obtained from the examined material is shown in Fig. 4. The nanohardness values decrease with the increasing peak indentation test load for ZE41 Mg alloy. On the other hand, in the Ce-doped alloys, nanohardness values increase with increasing peak indentation test load. The H_{N} is a function of the applied load at low peak indentation test loads, where there is no constant value for the hardness (H_{LD}; load-dependent hardness). At high-peak indentation test loads, the hardness is constant with respect to indentation test load and a well-defined hardness value exists (H_{LI}; load-independent hardness). H_{LI} has also been referred to as the "true" hardness in some literature. If the hardness values decrease with the increasing indentation test load, this behavior is called indentation size effect. Conversely, if the hardness increases, this behavior is called reverse indentation size effect [11–13].

The Hays-Kendall model (HK) [16] is applied to analyze the nanohardness data on the ZE41 Mg alloys. In this model authors have proposed that a minimum

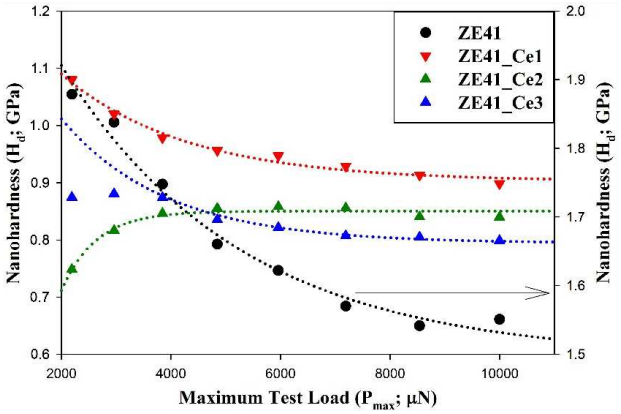

Fig. 4. Nanohardness variation as a function of test load.

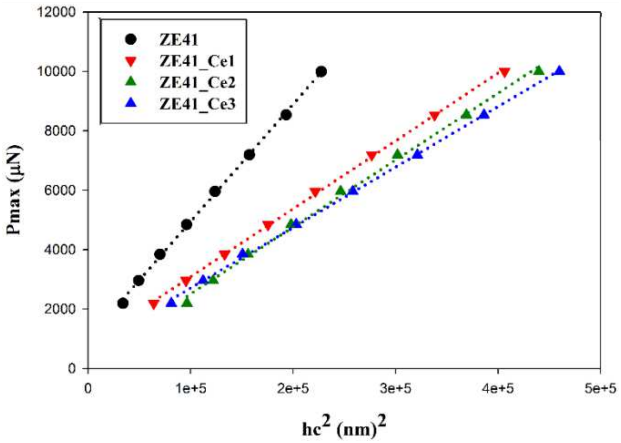

Fig. 5. Plots of $P_{\max}$ vs. h_{c}^2 for ZE41 Mg alloys.

applied test load W (test specimen resistance) is necessary to initiate plastic deformation, below which only elastic deformation occurs [17]. According to this model, effective load is calculated by

$$P_{\mathrm{effective}} = (P_{\max} - W) = K_1 h_{\mathrm{c}}^2, \tag{7}$$

$$H_{\mathrm{HK}} = 0.408\frac{(P_{\max} - W)}{h_{\mathrm{c}}^2} = 0.0408 D_1, \tag{8}$$

where W is the sample resistance pressure (or Newtonian resultant pressure), which represents the minimum load that causes an indentation, K_1 is a constant and $(P_{\max} - W)$ is an effective indentation load. Replacing $P_{\max}$ in Eq. (1) by $(P_{\max} - W)$, one gets an equation for the load-independent (or true) hardness (Eq. (8)). From the Eq. (7), a plot of $P_{\max}$ versus h_{c}^2 yields a straight line where W and K_1 parameters can easily be calculated from the intersection of the curve. Such a plot for ZE41 Mg alloys is shown in Fig. 5. The correlation coefficient r^2 for the sample is 0.999, implying that Eq. (7) provides a satisfactory description of the indentation data for the examined test materials. Load-independent hardness values, calculated using the Hays-Kendall model, H_{HK}, are given in Table II. The nanohardness value is very close to the plateau region (Fig. 4).

TABLE II

Best fit parameters and analysis results according to Hays-Kendall model [16].

Sample name	a_1 [μN/nm^2]	W [μN]	H_{HK} [GPa]	H_{LI} [GPa]
ZE41	0.0395	991.587	1.611	1.551
ZE41Ce1	0.0229	800.279	0.934	0.898
ZE41Ce2	0.0225	258.0750	0.918	0.839
ZE41Ce3	0.0204	668.9684	0.832	0.799

4. Conclusions

Effects of Ce as an additive in a mechanical alloying process of ZE41 alloys were investigated for the first time. Analysis of the results led to the following conclusions:

1. Experimental results show that measured hardness displays the peak load dependence. Load-independent hardness was calculated by Hays-Kendall approach. Load-independent hardness values are 1.551, 0.898, 0.839 and 0.799 GPa for ZE41, ZE41Ce1, ZE41Ce2 and ZE41Ce3, respectively.

2. From the XRD data it is found that as the Ce content increased, the crystallite sizes have also increased from 57.06 to 75.16 nm. On the other hand, the hardness of the alloys has decreased with the increasing Ce content.

3. It was found that Ce-doping modifies the microstructure and hardness, depending on the Ce amount.

Acknowledgments

This work was partially supported by the Scientific and Technological Research Council of Turkey (TUBİTAK) with Grant No: 213M699, and the Turkish State Planning Organization (DPT) with project no. 2010K121220 and it is also supported by the Scientific Research Commission of Mustafa Kemal University (BAP) (Project No: 10741, and 12880).

References

[1] F.H. Froes, D. Eliezer, E. Aghion, *JOM* **50**, 30 (1998).

[2] M. Gupta, N.M.L. Sharon, *Magnesium Alloys and Magnesium Composites*, John Wiley & Sons, New Jersy 2011.

[3] G.I. Rosen, G. Segal, A. Lubinsky, *Materials Sci. Forum* **488–489**, 509 (2005).

[4] C. Suryanarayana, *Prog. Mater. Sci.* **46**, 1 (2001).

[5] C. Suryanarayana, in: *Powder metal technologies and applications. ASM Handbook*, ASM International, Materials Park 1998, Vol. 7., p. 80.

[6] M.L.B. Palacio, B. Bhushan, *Mater. Charact.* **78**, 1 (2013).

[7] S. Lee, B.G. Choi, D. Choi, H.S. Park, *J. Membr. Sci.* **451**, 40 (2014).

[8] S.R. Jian, G.J. Chen, W.M. Hsu, *Materials* **6**, 4505 (2013).

[9] S.R. Jian, Y.Y. Lin, W.C. Ke, *Sci. Adv. Mater.* **5**, 7 (2013).

[10] S.R. Jian, Y.H. Lee, *J. Alloy. Compd.* **587**, 313 (2014).

[11] A.E. Ozmetin, O. Sahin, E. Ongun, M. Kuru, *J. Alloy. Compd.* **619**, 262 (2015).

[12] W.C. Oliver, G.M. Pharr, *J. Mater. Res.* **7**, 1564 (1992).

[13] O. Sahin, O. Uzun, M. Sopicka-Lizer, H. Gocmez, U. Kolemen, *J. Phys. D: Appl. Phys.* **41**, 035305 (2008).

[14] F. Haluk Ertsak, M.Sc. Thesis, Mustafa Kemal University, 2015.

[15] O. Sahin, İ. Demirkol, H. Göcmez, M. Tuncer, H. Ali Cetinkara, H. Salih Güder, E. Sahin, A. Rıza Tuncdemir, *Acta Phys. Pol.* **123**, 296 (2013).

[16] C. Hays, E.G. Kendall, *Metallography* **6**, 275 (1973).

[17] O. Şahin, O. Uzun, U. Kölemen, N. Uçar, *Material Characterization* **59**, 729 (2008).